Chapter 4

Proliferation Control of Human Lymphocytes with Ribozyme-Based Regulatory Systems

Partially adapted, with permission, from Chen, Y.Y., Jensen, M.C., & Smolke, C.D. Genetic control of mammalian T-cell proliferation with synthetic RNA regulatory systems. *Proc Natl Acad Sci USA* **107**, 8531–8536 (2010).

Abstract

Cellular immunotherapy utilizing the adoptive transfer of antigen-specific lymphocytes has achieved clinical success in the treatment of some virus-associated malignancies and cancers, particularly metastatic melanoma. However, objective clinical response from adoptive cell therapy is strongly correlated with the persistence of transferred cells in the patient, and the ability to regulate the proliferative response of human lymphocytes is critical to the safety and efficacy of adoptive immunotherapy. We have demonstrated that ribozyme-based regulatory systems are capable of drug-responsive control over T-cell proliferation in mouse models. Here, we demonstrate the application of ribozyme-based regulatory systems to proliferation control in human lymphocytes.

Given the central importance of human cells in immunotherapy and other applications in health and medicine, the ability to characterize and optimize new RNA-based control devices directly in human cells can greatly facilitate the development of gene-regulatory systems for clinical use. The human natural killer (NK) cell line NK-92, a candidate for adoptive cell therapy, is evaluated here as a model cell line for RNA-based device development. We verify the ability to reduce gene expression by 25%—and recover 18% of the expression in response to ligand addition—with only one copy of a theophylline-responsive ribozyme ON switch in NK-92 cells. However, we also demonstrate the unsuitability of NK-92 cells as a human cellular host for the characterization and optimization of novel RNA-based regulatory systems due to the inability to execute rapid and efficient genetic manipulation in this cell line.

Primary human central memory T (T_{CM}) cells represent another class of human lymphocytes currently under intensive investigation for clinical use. Here, we describe the generation of primary human T_{CM} cells stably expressing ribozyme switch systems using protocols readily adaptable to clinical-grade manufacturing standards. Engineered T_{CM} cells are shown to express the proper surface receptors for therapeutic applications, and the cell population can be effectively controlled with the use of the thymidine kinase suicide gene. A ribozyme-based regulatory system capable of modulating the production of the proliferative cytokine interleukin-15 (IL-15) is shown to function robustly in primary human T_{CM} cells, leading to a 24% increase in cell survival and a 54% reduction in apoptosis in response to theophylline treatment in a bulk, unsorted, lentivirally transduced T_{CM} population. These results highlight the portability of ribozyme-based control devices across organisms and demonstrate the applicability of ribozyme switch systems to the regulation of functional outputs in human cells suitable for clinical applications.

Introduction

Adoptive immunotherapy is a promising method for targeted treatment of virus-associated malignancies[1-4] and various cancers[5-8]. Unlike conventional cancer treatment strategies such as chemotherapy and radiation therapy, which are characterized by substantial off-target toxicities, the adoptive transfer of antigen-specific lymphocytes can precisely deliver therapeutic payloads to targeted tumors[9, 10]. A critical task in the development of adoptive immunotherapy is the identification of suitable lymphocyte lineages and manipulation methods to generate safe and potent candidates for clinical applications. Numerous types of lymphocytes have been evaluated as therapeutic candidates with varying degrees of success[11-17]. Among these, antigen-specific $CD8^+$ T cell clones derived from T_{CM} cells[18, 19] and the established cell line NK-92[20] have shown exciting potential for clinical applications.

$CD8^+$ T cells can be derived from either naïve T cells or antigen-experienced memory T cells, the latter being divided into central memory (T_{CM}) and effector memory (T_{EM}) subsets. T_{CM} cells constitutively express CD62L and CCR7, which facilitate cellular extravasation and migration to lymph nodes. In contrast, the $CD62L^{low}/CCR7^-$ T_{EM} cells are found in both lymphoid and peripheral tissues[21]. While T_{EM} cells have been the dominant choice in early clinical studies due to their strong lytic capacity and high IFN-γ production levels, several recent studies have reported that T_{CM} cells may be superior to T_{EM} cells in both long-term persistence and anti-tumor effects[18, 22]. For instance, Riddell and colleagues showed that antigen-specific $CD8^+$ T cell clones derived from T_{CM} cells, but not from T_{EM} cells, could achieve long-term persistence and occupy

memory T cell niches in primates, suggesting T_{CM} cells as a promising candidate for adoptive T-cell therapy[19].

The transplantation of NK cells represents an alternative paradigm in cellular immunotherapy[23]. NK cells are large, granular lymphocytes whose cytotoxic activities are regulated by the balance of various activating and inhibitory signals. Recognition of non-self major histocompatibility complex (MHC) and binding to certain ligands on tumor cells can trigger the release of granzyme and perforin from NK cells[24]. Conversely, recognition of self MHC results in the inactivation of NK cells mediated by killer immunoglobulin-like receptors (KIRs)[25]. Researchers have navigated this intricate signal balance and reported graft-versus-leukemia effects with the transplantation of allogeneic NK cells into human leukocyte antigen (HLA)-mismatched hosts[26, 27]. NK-92 is an NK tumor cell line with cytotoxic activity against a wide range of cancer cells and has demonstrated efficacy against both xenografted human leukemia and malignant melanoma in SCID mouse models[20, 28, 29]. Significantly, NK-92 cells express very low levels of KIRs but retain perforin and granzyme B–mediated cytolytic activities toward cancer cells[30]. In addition, they display no cytotoxicity toward non-malignant allogeneic cells[29], making them uniquely suited for adoptive immunotherapy.

Despite the diversity of potential candidates, cellular immunotherapy is constrained by the fact that the long-term survival and cytotoxicity of lymphocytes are dependent on cytokines such as interleukin 2 (IL-2) and interleukin 15 (IL-15). For instance, primary T_{CM} cells require IL-15 to establish persistent T-cell memory *in vivo*[19, 31], and the cytotoxicity of NK-92 cells declines to approximately 10% three days after IL-2 removal[32]. As discussed in Chapters 1 and 3, the ability to integrate growth stimulatory

gene expression with tightly controlled genetic regulatory systems has the potential to greatly improve the safety and efficacy of cellular immunotherapy.

We have demonstrated T-cell proliferation control in mouse models using RNA-based regulatory systems (Chapter 3), yet the ability to generate engineered human lymphocytes with the stringent quality standards and rapid time scale required for clinical applications remains to be shown. Furthermore, although we have demonstrated that RNA-based control devices developed in yeasts can be effectively transported into mammalian cells, the ability to prototype and optimize new devices directly in human cells would allow more efficient construction of RNA-based regulatory systems suitable for applications in health and medicine. To establish a protocol for developing regulatory systems that can readily interface with clinical applications, we investigated the NK-92 cell line's suitability as a model host for the characterization and optimization of ribozyme-based switch devices. As an established cell line, NK-92 cells have the advantage of being more readily available and easily cultured compared to primary human cells. These properties, coupled with the cell line's promise as a therapeutic agent, make NK-92 cells a potentially powerful host for the development of synthetic control systems. However, our studies show that NK-92 cells are not amenable to transient transfections and that detailed characterization of device performance in this cell line requires stable integration by lentiviral transduction, which significantly increases the time and resource consumption required for device optimization and renders NK-92 cells unsuited for high-throughput developmental work. Nevertheless, we demonstrate that ribozyme switch devices are capable of gene expression knockdown in NK-92 cells,

indicating that ribozyme-based regulatory systems may be useful in the functional control of NK-92 cells as a candidate for cellular immunotherapy.

Furthermore, we examine the performance of ribozyme-based regulatory systems in primary human T_{CM} cells, which have shown promise in adoptive T-cell therapy. Here, we report drug-responsive regulation of both gene expression and cell fate in T_{CM} cells using ribozyme switch devices. We describe the generation of engineered T_{CM} cells using protocols readily adaptable to clinical-grade manufacturing practices and demonstrate the effective regulation of functional output. Although we have been unable to identify a human lymphocyte cell line suitable for rapid characterization and optimization of ribozyme-based regulatory systems, our results show that ribozyme switch devices prototyped in yeast and optimized in a mouse T-cell line are functional in both established and primary human lymphocytes. This model of developing regulatory systems in progressively more complex cellular organisms for eventual applications in human cells may inform future work on the development of synthetic RNA-based regulatory systems.

Results

Transfection Optimization in NK-92 Cell Line. Both primary lymphocytes and established cell lines have been examined as candidates for adoptive immunotherapy. While each cell type has advantages over the other, established cell lines are more readily available and easily cultured. Furthermore, established cell lines generally have higher growth rates and more stable phenotypes compared to primary cells, whose phenotypic outcome can be highly sensitive to procedural details in the isolation and *in vitro* expansion protocols[33]. For these reasons, established cell lines such as NK-92 are potentially well suited for the rapid characterization and optimization of control devices in the development of synthetic gene regulatory systems.

NK-92 cells are IL-2-dependent and are therefore not fully transformed. This cytokine dependence has limited the therapeutic efficacy of NK-92 cells, but it also presents an opportunity for engineered proliferation control using RNA-based regulatory systems. Specifically, viability as a functional output can serve as a useful tool for the evaluation of control devices. We examined the sensitivity of NK-92 cells to various small-molecule ligands and verified that this cell line is equally or more robust than CTLL-2 cells in response to almost all of the ligands tested (Appendix 2), supporting NK-92 as a potentially useful host for the development of ligand-responsive regulatory systems. To examine the portability of ribozyme-based regulatory systems to NK-92 cells, we attempted to characterize previously described constructs (pIL2-based plasmids, Chapter 3) by transient transfection. However, NK cells are known to be highly resistant to transfection[34], and the NK-92 cell line also proved intransigent to commercially available electroporation protocols purportedly optimized for NK-92 transfection.

Electroporation of GFP-encoding plasmids into NK-92 cells was performed using the Amaxa Nucleofector Kit R following manufacturer's protocols, and results show essentially zero transfection efficiency (as defined by the percent of all viable cells that are fluorescent above background levels) for all plasmids tested except for the pmaxGFP control plasmid supplied by the electroporation kit manufacturer Amaxa (Figure 4.1).

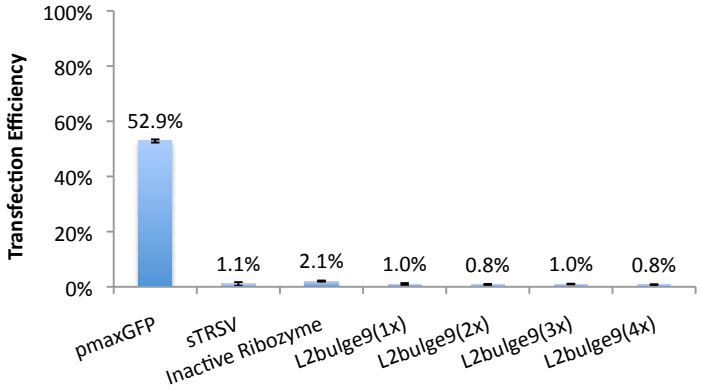

Figure 4.1. NK-92 cells cannot be effectively transfected by electroporation with DNA plasmids based on the pIL2 expression vector. NK-92 cells were transfected using an Amaxa Nucleofector II and the reagent kit and electroporation protocol optimized for NK-92 cells. The control plasmid, pmaxGFP, supplied by Amaxa was included as a positive control. pIL2-based plasmids expressing ribozyme constructs in the 3' UTR of the *egfp-t2a-il2* fusion gene from an EF1α promoter failed to transfect NK-92 cells. All plasmids other than pmaxGFP were prepared from DH10B cells using the Promega Wizard Plus SV Miniprep kit. Transfection efficiency was measured by the percent of total viable cells that are fluorescent. Reported values are the mean of duplicate samples ± s.d.

Several factors may have contributed to the observed difference in transfection efficiencies. First, expression of the reporter construct in pmaxGFP is driven by the cytomegalovirus (CMV) promoter while expression from the pIL2-based plasmids is driven by the elongation factor one alpha (EF1α) promoter. The two promoters exhibit different strengths in different cell types[35, 36] and may have caused the disparate transfection efficiencies observed in NK-92 cells. Second, the pmaxGFP plasmid was supplied by Amaxa and was therefore prepared separately from the other plasmids tested. Differences in plasmid purification methods may have affected transfection efficiencies. Third, the fluorescent protein encoded by pmaxGFP is derived from the copepod

Pontellina plumata and has significantly higher fluorescence intensity compared to the EGFP-T2A-IL2 fusion protein encoded by the other plasmids presented in Figures 4.1 (see Supplementary Text 3.1 and Supplementary Figure 4.1 for fluorophore comparisons). The relatively weak intensity of the fusion protein may have contributed to the low transfection efficiencies observed from plasmids encoding this fluorescent reporter. Finally, the pmaxGFP vector may possess yet-unidentified properties that enhance the expression of its encoded transgene. We performed additional electroporation studies to examine each of these factors.

To evaluate the effect of promoter strength, we inserted the *egfp-t2a-il2* fusion transgene into pcDNA3.1(+) and pcDNA5/FRT—two of the most commonly used mammalian expression vectors with the same CMV promoter as the pmaxGFP plasmid—and compared them against pmaxGFP. Results indicate that while pmaxGFP consistently achieves high transfection efficiency, the pcDNA3.1(+)- and pcDNA5/FRT-based plasmids are ineffective in transfecting NK-92 cells, suggesting that promoter strength is not the sole contributor to transfection efficiency in this cell line (Figure 4.2).

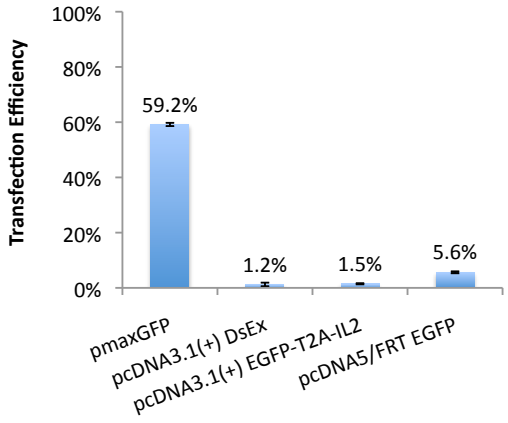

Figure 4.2. NK-92 cells cannot be effectively transfected by electroporation with DNA plasmids based on the pcDNA3.1(+) and pcDNA5/FRT expression vectors. NK-92 cells were transfected as described in Figure 4.1. pcDNA3.1(+)- and pcDNA5/FRT-based plasmids expressing dsRed-Express (DsEx), EGFP-T2A-IL2, or EGFP alone from a CMV promoter were ineffective at transfecting NK-92 cells. All plasmids other than pmaxGFP were prepared from DH10B cells using the Promega Wizard Plus SV Miniprep kit. Data are reported as described in Figure 4.1.

We next investigated whether plasmid preparation methods affect transfection efficiency. The pmaxGFP plasmid was transformed into two electrocompetent *Escherichia coli* strains, DH10B and DH5α, and plasmids were prepared from overnight liquid cultures using three different commercially available plasmid purification kits (Promega Wizard Plus SV Miniprep, Promega Pure Yield Miniprep, and Qiagen EndoFree Maxiprep). Results show that transfection efficiency is dependent on both the bacterial cell strain and the plasmid preparation method used, with DH10B and the Qiagen EndoFree Maxiprep kit being the optimum combination among those tested (Figure 4.3A). However, a pcDNA3.1(+)-based plasmid expressing the EGFP-T2A-IL2 fusion protein prepared from DH10B cells using the Qiagen kit still failed to transfect NK-92 cells (Figure 4.3B), indicating that additional requirements must be met to achieve efficient transfection.

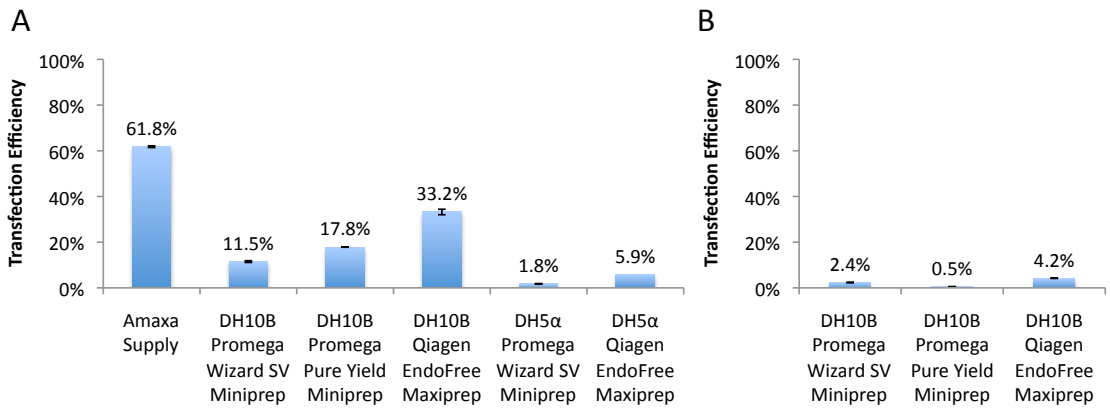

Figure 4.3. Appropriate bacterial strain and purification method used to prepare DNA plasmids are necessary but not sufficient for achieving high transfection efficiency in NK-92 cells. (A) The pmaxGFP plasmid was transformed into both DH10B and DH5α strains of *E. coli* and plasmids were purified from overnight liquid cultures using the Promega Wizard Plus SV Miniprep kit, the Promega Pure Yield Miniprep kit, or the Qiagen EndoFree Maxiprep kit. Plasmids purified from DH10B cells using the Qiagen kit showed the highest transfection efficiency among test samples but were still less efficient than control plasmids supplied directly by Amaxa. (B) A pcDNA3.1(+)-based plasmid expressing *egfp-t2a-il2* from a CMV promoter was unable to achieve high transfection efficiency regardless of the plasmid purification methods used. Transfection efficiency values are reported as in Figure 4.1.

We next investigated whether a stronger fluorophore expressed from the pcDNA3.1(+) vector could achieve higher efficiencies. As shown in Figure 4.2, electroporation with a pcDNA3.1(+)-based plasmid encoding the weak reporter EGFP-T2A-IL2 failed to generate any appreciable fluorescent population. In contrast, cells electroporated with a pcDNA3.1(+)-based plasmid encoding a stronger reporter, EGFP alone, showed a 19% $EGFP^+$ population (Figure 4.4A), suggesting the low percent $EGFP^+$ seen with previously tested plasmids could be artificially low due to weak fluorescence intensity rather than low transfection efficiencies. These results also indicate that NK-92 cells may exhibit lower expression levels overall compared to cell lines such as CTLL-2 and HEK, thus requiring stronger fluorophores for effective signal detection by flow cytometry.

In contrast to the pcDNA3.1(+)-based plasmid, the pcDNA5/FRT-based plasmid expressing EGFP showed significantly lower transfection efficiency (7%) and fluorescence intensity (Figure 4.4A, B), indicating that a strong fluorophore alone is insufficient to achieve high transgene expression in NK-92 cells. We hypothesized that the pmaxGFP plasmid backbone has unique properties that enhance the expression of transgenes encoded by this plasmid. To verify, we replaced the maxGFP reporter in pmaxGFP with the weaker EGFP-T2A-IL2 fusion protein to create the "pmaxGFP EGFP-T2A-IL2" construct and measured both transfection efficiency and fluorescence intensity from transiently transfected samples. Results show that while EGFP-T2A-IL2 has a lower fluorescence intensity compared to both maxGFP and EGFP as expected (Figure 4.4B), pmaxGFP EGFP-T2A-IL2 achieved higher transfection efficiency (33.2%, Figure 4.4A) compared to pcDNA3.1(+)-based plasmids expressing either EGFP-T2A-

IL2 (1.5%, Figure 4.2) or EGFP (18.6%, Figure 4.4A). These results suggest that the vector backbone has a stronger influence over transfection efficiency than the specific protein being expressed. It should be noted that the EGFP-T2A-IL2 fusion protein yielded the lowest intensity among all the samples shown in Figure 4.4 despite having the second largest GFP^+ population, indicating that the transfection efficiency measured is not completely dependent on fluorophore strength. However, fluorescence intensity is affected by transfection efficiency, as indicated by the fact that the pcDNA5/FRT EGFP construct showed markedly lower intensity compared to the pcDNA3.1(+) EGFP construct despite having the same fluorophore as a reporter protein (Figure 4.4B).

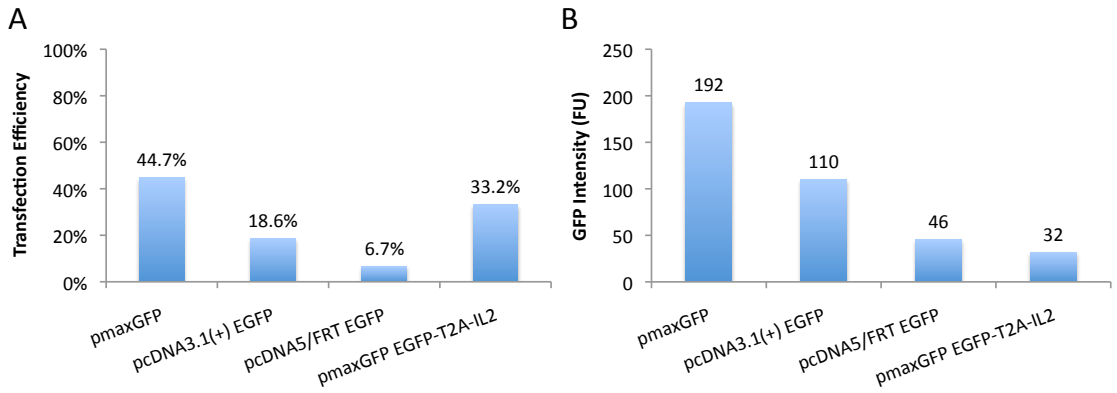

Figure 4.4. Vector backbone has greater influence on transfection efficiency in NK-92 cells than the specific fluorophore encoded by the vector. (A) Plasmids encoding variants of GFP in different vector backbones show varying degrees of transfection efficiency, with the pmaxGFP vector achieving the highest transfection efficiency regardless of the relative strengths of the fluorophores being expressed. (B) The fluorescence intensity expressed by transiently transfected NK-92 cells is dependent on both transfection efficiency and the strength of the particular fluorophore used. Transfection efficiency was measured by the percent of total viable cells that are fluorescent. Reported GFP intensity is the geometric mean fluorescence of the viable, GFP^+ gated population.

Taken together, the results suggest the optimized system for electroporating NK-92 cells requires pmaxGFP-based vectors prepared from DH10B cells using the Qiagen EndoFree Maxiprep kit. Furthermore, a strong fluorophore serving as reporter protein would facilitate flow cytometry analysis and achieve higher measurable levels of transfection efficiency. Since viability cannot be evaluated after gating for transfected

populations (because transfected populations are defined as viable, fluorescent cells), viability measurements must be based on the entire culture sample. As a result, the accuracy of viability measurements is strongly dependent on having high transfection efficiencies in all samples. Our transient transfection results indicate that transfection efficiency is limited to approximately 35% using the EGFP-T2A-IL2 fusion protein as the reporter, and such low transfection levels prevent accurate quantification of viability knockdown. As such, NK-92 cells cannot serve as a robust human cell model for the characterization and optimization of T-cell proliferation control systems. However, as a potential candidate for immunotherapy, NK-92 cells may still benefit from the regulatory functions of ribozyme-based control systems. Therefore, we reconfigured the characterization system and inserted ribozyme switch devices behind the *maxgfp* gene in pmaxGFP, thus permitting the quantification of gene expression regulation by fluorescence measurements.

Ribozyme Switches Achieve Gene Expression Knockdown in NK-92 Cells. To evaluate the performance of ribozyme-based regulatory systems in NK-92 cells, we performed transient transfections of a construct encoding one copy of the theophylline-responsive ON switch L2bulge9 in the 3' UTR of the *maxgfp* gene. Constructs encoding an inactive ribozyme and the non-switch, fully active satellite RNA of tobacco ringspot virus (sTRSV) hammerhead ribozyme were included as positive (maximum expression) and negative (minimum expression) controls, respectively. The unmodified pmaxGFP plasmid was also included for comparison. Percent GFP expression was calculated by normalizing to the inactive ribozyme control, and results indicate both gene expression

knockdown and theophylline-responsive ON switch activity by the L2bulge9 switch (Figure 4.5A). However, unlike the device performance observed in CTLL-2 cells (Figure 3.2), the sTRSV ribozyme also appears to respond to theophylline as an ON switch in NK-92 cells (Figure 4.5A).

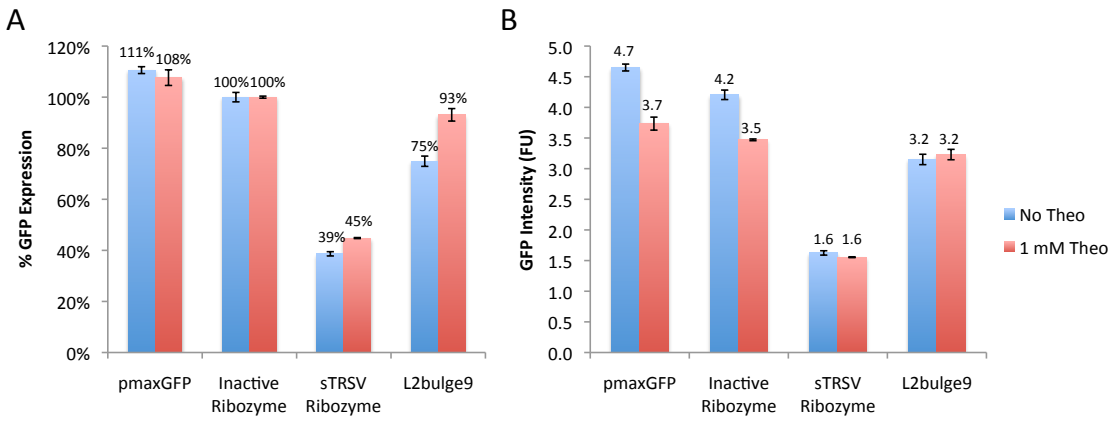

Figure 4.5. A ribozyme switch device is capable of gene expression knockdown in NK-92 cells. NK-92 cells were transfected as described in Figure 4.1 with plasmids constructed by inserting various ribozymes in the 3' UTR of the *maxgfp* gene in pmaxGFP and cultured in the absence or presence of 1 mM theophylline. (A) GFP expression levels normalized to the inactive ribozyme control show theophylline-responsive ON switch behavior by the sTRSV ribozyme and the L2bulge9 ribozyme switch. (B) Theophylline addition has no impact on the absolute fluorescence intensity of sTRSV ribozyme and L2bulge9 samples but results in decreased fluorescence in the pmaxGFP (no ribozyme control) and inactive ribozyme control samples.

Closer inspection of transfection results reveals that the absolute fluorescence levels of the sTRSV ribozyme and L2bulge9 samples remained constant while those of the inactive ribozyme control and pmaxGFP samples decreased in response to theophylline addition (Figure 4.5B). Although non-specific effects of theophylline on gene expression and fluorescence intensity have been observed in previous studies in CTLL-2 and HEK cells, these effects were proportional across different devices and were corrected by normalizing to the inactive ribozyme control. The behavior observed in NK-92 cells appears to be unique and not fully accounted for by the normalization scheme employed. Therefore, we conclude that the ribozyme device is capable of gene expression

knockdown in NK-92 cells, but ligand-responsiveness cannot be confirmed in this cell line.

Stable Integration of Ribozyme-Based Regulatory Systems in Primary Human T_{CM} Cells. The use of primary human T cells in adoptive immunotherapy is well established[37], and primary human T_{CM} cells show great promise as an immunotherapeutic agent given their ability to achieve long-term persistence in primates in the presence of IL-15[19]. To demonstrate the ribozyme-based regulatory system's portability to human T lymphocytes and translatability to clinical applications, we stably integrated ribozyme-based regulatory systems into primary human T_{CM} cells by lentiviral transduction. T_{CM} cells were isolated from peripheral blood mononuclear cells (PBMCs) by magnetic sorting using the autoMACS system (Miltenyi), a method chosen for its ready adaptation to clinical-grade manufacturing processes using the CliniMACS system (Miltenyi). PBMCs were depleted of $CD4^+$, $CD14^+$, and $CD45RA^+$ populations and subsequently enriched for $CD62L^+$ cells. The isolated T_{CM} cells were then transduced with lentiviral vectors encoding the *cd19-tk-t2a-il15* transgene coupled to three copies of the L2bulge9 switch or to an inactive ribozyme.

To verify stable integration of the regulatory system, T_{CM} cells transduced with ribozyme switch systems were tested for sensitivity to ganciclovir conferred by the mutant HSV-1 thymidine kinase (*tk*) gene. Transduced cells cultured in the presence of 5 μM ganciclovir showed decreased viability and growth while parental T_{CM} cells showed no sensitivity to the drug, confirming stable construct integration and demonstrating that the suicide switch programmed into the regulatory system as a safety mechanism is fully

functional (Figure 4.6). To verify that the transduced T_{CM} cells retained phenotypes critical for therapeutic functions, we performed surface antibody staining for the T-cell receptor (TCR), CD4, and CD8. As anticipated, transduced T_{CM} cells retained TCR and CD8 expression and remained $CD4^-$ (Figure 4.7). These results indicate that engineered T_{CM} cells stably expressing the ribozyme-based regulatory system can be efficiently generated without altering critical cell phenotypes.

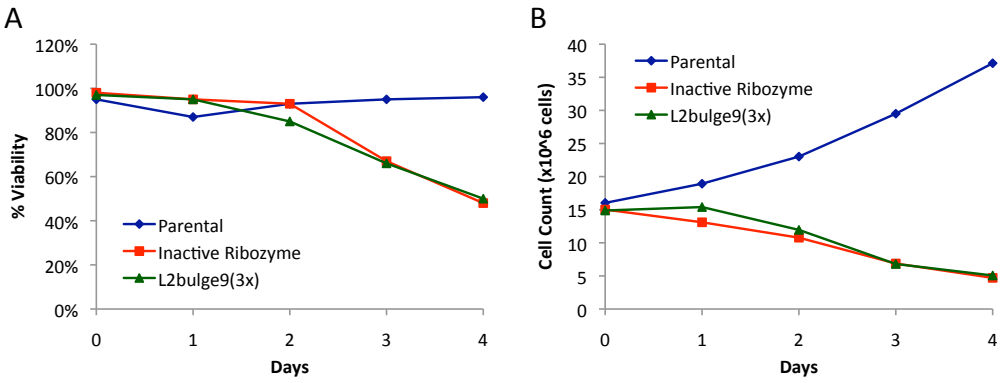

Figure 4.6. The suicide-gene safety switch programmed in ribozyme-based proliferation control systems is functional in primary human T_{CM} cells. T_{CM} cells lentivirally transduced with constructs encoding the *cd19-tk-t2a-il15* gene and ribozyme switches were cultured in the presence of 5 μM ganciclovir for four days. Compared to parental T_{CM} cells that do not express thymidine kinase (tk), the transduced cells show reduced (A) % viability and (B) total viable cell count in response to ganciclovir treatment.

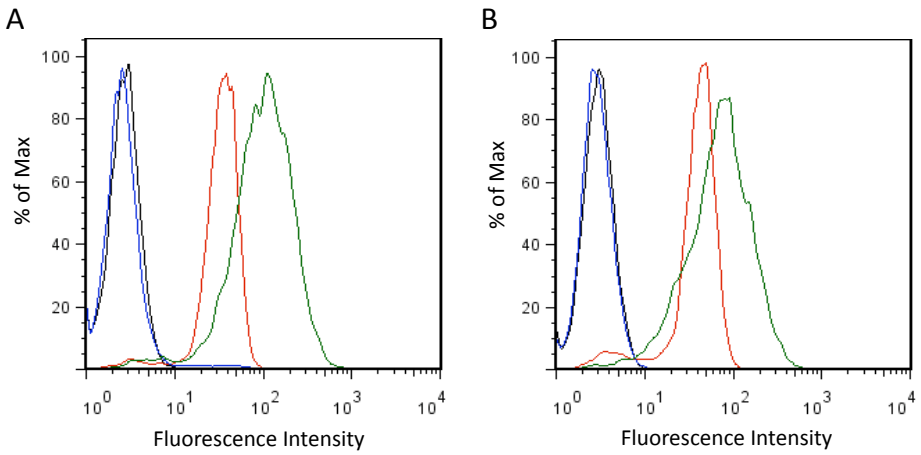

Figure 4.7. T_{CM} cells stably expressing ribozyme switch systems exhibit the proper phenotype for therapeutic applications. T_{CM} cells lentivirally transduced with constructs encoding the *cd19-tk-t2a-il15* gene and (A) the inactive ribozyme control or (B) the theophylline-responsive L2bulge9(3x) ribozyme switch are shown to be $TCR^+/CD4^-/CD8^+$ by surface antibody staining. Black, isotype control; red, TCR; blue, CD4; green, CD8.

Ribozyme Switches Enable Proliferation Control in Engineered T_{CM} Cells. Since short production timelines and streamlined processing are critical in clinical applications, we conducted regulatory performance evaluations on bulk transduced, unsorted T_{CM} populations to examine the robustness of the regulatory system under no population refinement. Transduced cells were cultured in the presence and absence of 500 μM theophylline for five days, with daily monitoring of CD19 levels and cell viability. Cells expressing L2bulge9 show up to 15% increase in CD19 expression levels (Figure 4.8A), 24% increase in the live cell population (Figure 4.8B), and 54% reduction in the apoptotic cell population (Figure 4.8C) in the presence of theophylline compared to the inactive ribozyme control, indicating drug-responsive ON switch behavior in gene expression and cell growth. The measured change in CD19 expression is comparable to that observed in bulk CTLL-2 stable cell lines (Supplementary Figure 3.2), and the shift in population distribution between live and apoptotic cells supports that the regulatory system is effective in controlling the fate of primary human T_{CM} cells.

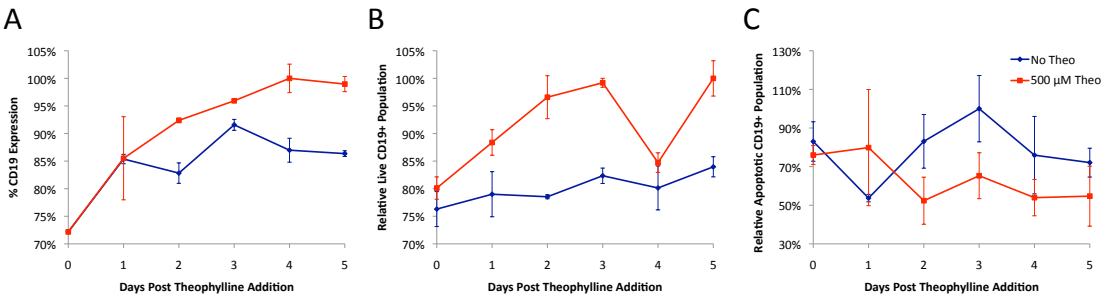

Figure 4.8. The ribozyme switch system effectively regulates gene expression and cell fate in primary human T_{CM} cells. (A) CD19 expression levels are elevated in the presence of theophylline. The populations of cells that are (B) live and $CD19^+$ or (C) apoptotic and $CD19^+$ indicate an increase in live cells and decrease in apoptotic cells in response to theophylline. Values for the L2bulge9(3x) sample are normalized to those of the inactive ribozyme control cultured at the same theophylline concentration. Reported values are mean ± s.d. from triplicate samples. The highest level is set to 100%.

Discussion

The ability to regulate gene expression and cell fate in primary human T cells using compact, programmable control systems is a significant step toward more effective adoptive immunotherapy. Multiple clinical trials have shown that the long-term persistence of adoptively transferred tumor-targeting cells is tightly correlated with the objective response rate[38]. However, maintaining and controlling the survival and expansion of transferred cells *in vivo* remain challenging. As discussed in Chapter 3, we have demonstrated that ribozyme-based regulatory systems can effectively control the proliferation of engineered T cells in mouse models by modulating the expression of growth-related cytokines in a ligand-responsive manner. In this work, we expand the functional range of the ribozyme-based regulatory systems into human cells. We seek to both identify a suitable human lymphocyte for the rapid characterization and optimization of RNA-based control devices and demonstrate the ligand-responsive gene-regulatory capabilities of ribozyme-based systems in established and primary human cells.

Similar to engineered mechanical systems, gene-regulatory systems consisting of biologically engineered control devices are products of a development process that encompasses initial design, prototyping, characterization, optimization, and final implementation. As discussed in Chapter 2, most of the RNA-based control devices published to date have been developed in model organisms such as yeasts and bacteria, primarily due to the high growth rate, ease of culture maintenance, and wide range of genetic manipulation tools available to these organisms. These characteristics enable rapid prototyping, characterization, and optimization of new devices. However, additional modifications are likely necessary during the implementation stage if the

desired application required different cellular hosts than the model organisms used for initial device development. An alternative strategy is to perform the development process in either the application's required cell type or a closely related organism. In the context of cellular immunotherapy, the goal is to implement regulatory systems capable of proliferation control in human lymphocytes. To identify a cellular host suitable for the development of such RNA-based control devices, we sought human lymphocytes that fulfill the following criteria: ready availability, ease of culture, cytokine dependence for growth (to allow for proliferation control via modulation of cytokine production), and amenability to rapid and effective genetic manipulation.

NK-92 was the first established NK cell line to be tested in clinical trials and continues to be a promising candidate for therapeutic applications. Importantly, it satisfies the first three criteria listed above for an ideal host for the development of RNA-based control devices. As an established cell line, NK-92 is readily available from cell banks such as the American Type Culture Collection (ATCC) and can be cultured in commercially available media without the need for antigen stimulation. NK-92 cells are dependent on cytokines (IL-2 or IL-15) for growth, making it a suitable candidate for proliferation control by RNA-based modulation of cytokine expression. However, the genetic manipulation of NK-92 cells has been hampered by difficulties in achieving efficient transfection by both lipid-based and electroporation methods. Lentiviral transduction has shown greater success in achieving transient expression in NK-92 cells, but the stable expression of transgenes remains challenging in this cell line. Furthermore, viral transduction requires greater infrastructural investments and is significantly more time consuming than lipid-based or electroporation methods for transient studies. Here,

we examined various parameters in the electroporation of NK-92 cells and identified a specific expression vector (pmaxGFP) and plasmid purification method (from DH10B cells using Qiagen EndoFree Maxiprep kit) that are critical to efficient transfections. By constructing ribozyme-based regulatory systems using the identified expression vector, we confirmed the gene expression knockdown activity of a ribozyme switch in NK-92 cells. However, our studies also show that the efficiency of transient transfections in NK-92 cells is too low for accurate quantification of the regulatory systems' impacts on cell viability. The alternative strategy of stable integration by lentiviral transduction significantly increases the time and resources required to evaluate each control device, thus precluding NK-92 as a suitable host for the characterization and optimization of new devices.

In contrast to established cell lines such as NK-92, primary human T cells must be obtained from fresh donor blood supplies, require regular antigen stimulation for *in vitro* expansion, and have a limited lifetime. Furthermore, primary T cells are generally resistant to rapid genetic manipulation strategies such as lipid-based transfection and electroporation, making them unsuited for hosting development work on RNA-based regulatory systems. Nevertheless, primary human T cells represent the most common cell type for adoptive cell therapy, and primary human T_{CM} cells in particular have shown promise as therapeutic agents. Therefore, the ability to maintain and control the proliferation of primary human T_{CM} cells can greatly contribute to the improvement of cellular immunotherapy. Our work presents the successful generation of primary human T_{CM} cells that stably express ribozyme-based regulatory systems capable of drug-responsive modulation of functional outputs. The T_{CM} cells were prepared using

protocols that are readily adaptable to clinical-grade manufacturing standards, and the resulting engineered population exhibits proper phenotypes for therapeutic applications. Significantly, T_{CM} cells transduced with the ribozyme switch system show drug-responsive regulation of both gene expression and cell-fate decisions without population refinement, confirming the robustness of the regulatory system and suggesting the potential for further performance improvement via isolation of clonal populations with the optimal behavioral outputs.

The examination of NK-92 and T_{CM} cells presented in this work confirms that the ribozyme-based regulatory system can be applied across multiple cell types through diverse genetic manipulation methods, including lipid-based transfection (in HEK cells, Chapter 2), electroporation (in CTLL-2 cells, Chapter 3), and lentiviral transduction (in T_{CM} cells). This flexibility in integration method and versatility across established cell lines as well as primary human cells will likely be critical to the implementation of ribozyme-based regulatory systems in diverse applications. In this study we also demonstrate that neither NK-92 cells nor primary human T cells are ideal hosts for the rapid characterization and optimization of RNA-based control devices due to limitations in cell availability and culture maintenance requirements (for primary T cells) as well as difficulties in achieving rapid genetic manipulations (for both NK-92 and primary T cells). Although characterization results of ribozyme-based regulatory systems in NK-92 and T_{CM} cells demonstrate that control devices prototyped and optimized in model organisms (yeast in this case) can be efficiently implemented in higher organisms useful for end applications such as adoptive immunotherapy, continued effort on identifying a human cell type suitable for the development of RNA-based control devices will further

improve the development process of engineered gene regulatory systems. The need for ready availability and ease of culture suggests that established cell lines are more promising candidates than primary cells. For systems that do not require cytokine-dependent growth as a functional criterion, numerous human lymphocyte lines, such as the well-characterized Jurkat cells, could be evaluated for suitability in hosting the characterization and optimization of RNA-based control devices. Future work in this area will facilitate the development of new RNA-based regulatory systems that can readily interface with clinical and other downstream applications requiring the use of human cells.

Materials and Methods

Plasmid construction. All plasmids were constructed using standard molecular biology techniques[39]. All oligonucleotides were synthesized by Integrated DNA Technologies or the Stanford Protein and Nucleic Acid Facility. All constructs were sequence verified (Elim Biopharmaceuticals). Cloning enzymes, including restriction enzymes and T4 DNA ligase, were obtained from New England Biolabs, and DNA polymerases were obtained from Stratagene. Construction of pcDNA5/FRT- and pcDNA3.1(+)-based plasmids was described in Chapters 2 and 3, respectively. The ribozyme sTRSV was cloned into the vector pmaxGFP (Amaxa) by annealing 5'-phosphorylated oligos for the sTRSV ribozyme (sTRSV BglII-P Fwd, 5'PGATCTTCGAGGCGATCGCAAACAAAC AAAGCTGTCACCGGATGTGCTTTCCGGTCTGATGAGTCCGTGAGGACGAAAC AGCAAAAAGAAAAATAAAAATTTTTTTTTAATTAATCTTGGGCCGAGCT; sTRSV SacI-P Rev, 5'PCGGCCCAAGATTAATTAAAAAAAAATTTTTATTTTT

CTTTTTGCTGTTTCGTCCTCACGGACTCATCAGACCGGAAAGCACATCCGGTG ACAGCTTTGTTTGTTTGCGATCGCCTCGAA) and inserting into the restriction sites BglII and SacI in the vector. The inactive ribozyme sTRSV Ctrl was similarly constructed using forward primer sTRSV Ctrl BglII-P Fwd (5'PGATCTTCGAGGCGATCGCAAACAAACAAAGCTGTCACCGGATGTGCTTTC CGGTACGTGAGGTCCGTGAGGACAGAACAGCAAAAAGAAAAATAAAAATTT TTTTTTTAATTAATCTTGGGCCGAGCT) and reverse primer sTRSV Ctrl SacI-P Rev (5'PCGGCCCAAGATTAATTAAAAAAAAAATTTTTATTTTTCTTTTTGCTGTTCT GTCCTCACGGACCTCACGTACCGGAAAGCACATCCGGTGACAGCTTTGTTTGT TTGCGATCGCCTCGAA). The L2bulge9 ribozyme switch sequence was PCR amplified from previously constructed plasmids using forward primer BglII Pre-Rz Fwd (5'AATAAGATCTTCGAGGCGATCGC AA) and reverse primer SacI Post-Rz Rev (5'AATAGAGCTCGGCCCAAGATTAATTAA AA) and inserted into BglII and SacI in pmaxGFP. The *egfp-t2a-il2* fusion gene was cloned into pmaxGFP via the KpnI and XhoI sites, thereby replacing the original gene encoding maxGFP.

Derivation of T_{CM} cells from human PBMCs. 5 x 10^8 PBMCs were isolated from donor apheresis products, washed twice with 35 ml MACS buffer (2 mM EDTA and 0.5% BSA in PBS), resuspended in 1.5 ml MACS buffer. Washed cells were stained with 0.75 ml each of CD4, CD14, and CD45RA microbeads (Miltenyi Biotec), and depleted for CD4, CD14, and CD45RA using an autoMACS Separator (Miltenyi). Depleted cells were washed once with 35 ml MACS buffer, resuspended in 3.5 ml MACS buffer with 10.5 μl anti-CD62L DREG56-biotin antibody (City of Hope Center for Biomedicine and

Genetics), and incubated for 20 min in the dark at 4°C. Cells were washed twice with 35 ml MACS buffer and resuspended in 1.2 ml MACS buffer with 300 μl anti-biotin microbeads (Miltenyi). Cells were enriched for CD62L using an autoMACS Separator, placed in fresh RPMI 1640 media supplemented with 10% FBS and stored in a 37°C incubator.

Mammalian cell culture maintenance. Primary human T_{CM} cells were maintained in RPMI-1640 media (Lonza) supplemented with 10% heat-inactivated FBS (Hyclone). Cells were fed 50 U/ml IL-2 and 0.5 ng/ml IL-15 every 48 hr and maintained between 0.2 x 10^6 and 1.0 x 10^6 cells/ml. NK-92 cells were maintained in X-VIVO 20 media (Lonza) and fed 500 U/ml IL-2 every 48 hours. Cultures were maintained between 0.08 x 10^6 cells/ml and 0.4 x 10^6 cells/ml. T_{CM} cell count and viability measurements were performed using the Guava Personal Cell Analysis System following manufacturer's protocols.

DNA plasmid preparation. Plasmids were prepared from 5 ml overnight liquid cultures supplemented with the appropriate antibiotics and inoculated directly from frozen *E. coli* stocks. Promega Wizard Plus SV Miniprep, Promega Pure Yield Miniprep, and Qiagen EndoFree Maxiprep kits were used for DNA purification following manufacturers' protocols.

Transient transfection and fluorescence quantification. Transfection of NK-92 cells was performed with an Amaxa Nucleofector II and Nucleofector Kit R (Amaxa)

following manufacturer's protocols. Each electroporation sample contained 2 x 10^6 cells transfected with 3 μg of plasmid DNA. Fluorescence data were obtained 48 hours after transfection using a Quanta Cell Lab Flow Cytometer equipped with a 488-nm laser (Beckman Coulter). GFP and dsRed-Express were measured through 525/30-nm band-pass and 610-nm long-pass filters, respectively. Viability was gated based on side scatter and electronic volume, and only viable cells were included in fluorescence measurements. All fluorescence measurements were reported as the geometric mean intensity observed in the gated population. Transfection efficiency was measured by the percent of total population that is GFP^+ or dsRed-$Express^+$, depending on the plasmids used. To control for toxicity and other possible non-specific effects of transfection and input ligand molecules, cells transfected with an inactive (scrambled) hammerhead ribozyme and treated with the corresponding concentration of ligand molecule served as positive controls to which values from cells transfected with active ribozyme switches were normalized. The inactive ribozyme constructs provide controls for the maximum possible gene expression levels from the ribozyme-based regulatory systems. Ribozyme sequences are as reported in Chapter 3. Reported error bars indicate one standard deviation.

Lentivirus production. 5.0 x 10^6 293T cells were seeded in a final volume of 9 ml per 10-cm tissue culture plate and transfected with 1 ml solution containing vector DNA, 62 mM $CaCl_2$, and 1X HEPES buffered saline. Cells were washed twice with 5 ml 1X PBS without magnesium and calcium the following morning and fed 10 ml of complete DMEM with 60 mM sodium butyrate. At 24-, 48-, and 72-hr post transfection, viral

supernatants were harvested by centrifugation at 2,000 rpm for 10 min at 4°C and filtered through 0.45 μM vacuum filtration unit. Viral supernatants from all time points were pooled and mixed with ¼ volume of 40% PEG. After rotating overnight at 4°C, samples were centrifuged at 3,000 rpm for 20 min at 4°C and the supernatants discarded. Pellets were resuspended in 35 ml serum-free DMEM and ultracentrifuged at 24,500 rpm for 1.5 hr at 4°C. Resulting pellets were resuspended in 50 μl serum-free FBS and vortexed at 4°C for 2 hr. 10% FBS was added and the samples stored at –80°C until titering and use.

Lentiviral transduction of T_{CM} cells. 0.5 x 10^6 T_{CM} cells were seeded in a total volume of 500 μl per well in 48-well plate. 1.5 x 10^6 anti-CD3/anti-CD28 Dynabeads (Invitrogen) were washed with 1% heat-inactivated human serum in PBS (pH 7.4), resuspended in 500 μl T-cell media (RPMI 1640 supplemented with 10% heat-inactivated fetal bovine serum) containing 0.5 x 10^6 T_{CM} cells, and added to each of 2 wells in a 48-well plate. Each well was fed with 50 U/ml IL-2 and 0.5 ng/ml IL-15, infected with viruses at a multiplicity of infection (MOI) of 5, and treated with protamine sulfate at a final concentration of 5 μg/ml. The plate was centrifuged at 2100 rpm for 30 min at 32°C and incubated at 37°C for 4 hr. 500 μl of warm T-cell media was added to each well and the plate was incubated at 37°C. Cells were assayed by flow cytometry on day 8 post transduction and Dynabeads were removed on day 14 post transduction.

Surface antibody staining. Surface staining of T_{CM} and NK-92 cells was performed by washing 1 x 10^6 cells twice with 500 μl HBSS (Gibco), incubating with FITC- or PE-conjugated antibodies at the appropriate dilution in 50 μl HBSS for 15 min at 4°C in the

dark, washing twice with 500 μl HBSS, and analyzing on the flow cytometer. FITC and PE signals were excited by a 488-nm laser and detected through 525/30-nm and 575/30-nm band-pass filters, respectively, using a Quanta Cell Lab Flow Cytometer.

T_{CM} cell time-course study. T_{CM} cells transduced with the *cd19-t2a-il15*-L2bulge9(3x) or *cd19-t2a-il15*-inactive ribozyme constructs were stimulated with 100 x 10^6 PBMCs, 10 x 10^6 TM-LCLs, and 30 ng/ml OKT2 for each T75 flask and cultured under regular conditions for 12 days. On day 12 after stimulation, each cell line was washed twice with HBSS and used to seed 25-ml cultures at 0.45 x 10^6 cells/ml. Cell media were supplemented with either no theophylline or 500 μM theophylline, and no IL-2 or IL-15 was added. The CD19 expression level study was performed with duplicate cultures and the apoptosis staining study was performed with triplicate cultures. 500 μl of each culture was sampled every 24 hr for surface staining with PE-conjugated CD19 antibody (Beckman Coulter). For the apoptosis study, CD19-stained samples where subsequently stained with Pacific Blue-conjugated annexin V and SYTOX AAD dead cell stain (Invitrogen) following manufacturer's protocols. Fluorescence data were obtained using a Quanta Cell Lab Flow Cytometer with both a 488-nm laser and a UV arc lamp. Pacific Blue, PE, and SYTOX AAD were detected through 465/30-nm band pass, 575/30-nm band pass, and 610-nm long-pass filters, respectively. Percent CD19 expression was calculated by measuring the PE expression level of PE^+ gated cells and normalizing results of the L2bulge9(3x) sample by those of the inactive ribozyme sample cultured at the same theophylline concentration. Only SYTOX AAD^- cells were included in data analyses for the apoptosis study. The population of live $CD19^+$ cells was determined by

gating for annexin V^-/PE^+ cells and the population of apoptotic $CD19^+$ cells was determined by gating for annexin V^+/PE^+ cells. Relative population distribution was calculated by normalizing results of the L2bulge9(3x) sample to those of the inactive ribozyme sample cultured at the same theophylline concentration.

Acknowledgments

We thank C. Bautista and E. Ferkassian for technical assistance. This work was supported by the City of Hope's National Cancer Institute–Cancer Center Support Grant, the Alfred P. Sloan Foundation (fellowship to C.D.S.), and the National Institutes of Health (grant to C.D.S., RC1GM091298).

References

1. Riddell, S.R. et al. Restoration of viral immunity in immunodeficient humans by the adoptive transfer of T cell clones. *Science* **257**, 238-241 (1992).
2. Walter, E.A. et al. Reconstitution of cellular immunity against cytomegalovirus in recipients of allogeneic bone marrow by transfer of T-cell clones from the donor. *N Engl J Med* **333**, 1038-1044 (1995).
3. Rooney, C.M. et al. Infusion of cytotoxic T cells for the prevention and treatment of Epstein-Barr virus-induced lymphoma in allogeneic transplant recipients. *Blood* **92**, 1549-1555 (1998).
4. Bollard, C.M. et al. Cytotoxic T lymphocyte therapy for Epstein-Barr virus+ Hodgkin's disease. *J Exp Med* **200**, 1623-1633 (2004).

5. Brentjens, R.J. et al. Eradication of systemic B-cell tumors by genetically targeted human T lymphocytes co-stimulated by CD80 and interleukin-15. *Nat Med* **9**, 279-286 (2003).

6. Dudley, M.E. et al. Adoptive cell transfer therapy following non-myeloablative but lymphodepleting chemotherapy for the treatment of patients with refractory metastatic melanoma. *J Clin Oncol* **23**, 2346-2357 (2005).

7. Morgan, R.A. et al. Cancer regression in patients after transfer of genetically engineered lymphocytes. *Science* **314**, 126-129 (2006).

8. Park, J.H. & Brentjens, R.J. Adoptive immunotherapy for B-cell malignancies with autologous chimeric antigen receptor modified tumor targeted T cells. *Discov Med* **9**, 277-288.

9. Blattman, J.N. & Greenberg, P.D. Cancer immunotherapy: a treatment for the masses. *Science* **305**, 200-205 (2004).

10. June, C.H. Adoptive T cell therapy for cancer in the clinic. *J Clin Invest* **117**, 1466-1476 (2007).

11. Antony, P.A. et al. CD8+ T cell immunity against a tumor/self-antigen is augmented by CD4+ T helper cells and hindered by naturally occurring T regulatory cells. *J Immunol* **174**, 2591-2601 (2005).

12. Powell, D.J., Jr., Dudley, M.E., Robbins, P.F. & Rosenberg, S.A. Transition of late-stage effector T cells to CD27+ CD28+ tumor-reactive effector memory T cells in humans after adoptive cell transfer therapy. *Blood* **105**, 241-250 (2005).

13. Ahmed, N. et al. HER2-specific T cells target primary glioblastoma stem cells and induce regression of autologous experimental tumors. *Clin Cancer Res* **16**, 474-485 (2010).

14. Kobayashi, H., Tanaka, Y., Shimmura, H., Minato, N. & Tanabe, K. Complete remission of lung metastasis following adoptive immunotherapy using activated autologous gammadelta T-cells in a patient with renal cell carcinoma. *Anticancer Res* **30**, 575-579 (2010).

15. Kuci, S. et al. Efficient lysis of rhabdomyosarcoma cells by cytokine-induced killer cells: implications for adoptive immunotherapy after allogeneic stem cell transplantation. *Haematologica* (2010).

16. Merlo, A. et al. Virus-Specific Cytotoxic CD4+ T Cells for the Treatment of EBV-Related Tumors. *J Immunol* (2010).

17. Wang, L.X. & Plautz, G.E. Tumor-Primed, In Vitro-Activated CD4+ Effector T Cells Establish Long-Term Memory without Exogenous Cytokine Support or Ongoing Antigen Exposure. *J Immunol* (2010).

18. Klebanoff, C.A. et al. Central memory self/tumor-reactive CD8+ T cells confer superior antitumor immunity compared with effector memory T cells. *Proc Natl Acad Sci U S A* **102**, 9571-9576 (2005).

19. Berger, C. et al. Adoptive transfer of effector CD8+ T cells derived from central memory cells establishes persistent T cell memory in primates. *J Clin Invest* **118**, 294-305 (2008).

20. Klingemann, H.G., Wong, E. & Maki, G. A cytotoxic NK-cell line (NK-92) for ex vivo purging of leukemia from blood. *Biol Blood Marrow Transplant* **2**, 68-75 (1996).

21. Roberts, A.D. & Woodland, D.L. Cutting edge: effector memory CD8+ T cells play a prominent role in recall responses to secondary viral infection in the lung. *J Immunol* **172**, 6533-6537 (2004).

22. Wherry, E.J. et al. Lineage relationship and protective immunity of memory CD8 T cell subsets. *Nat Immunol* **4**, 225-234 (2003).

23. Klingemann, H.G. Natural killer cell-based immunotherapeutic strategies. *Cytotherapy* **7**, 16-22 (2005).

24. Cantoni, C. et al. NKp44, a triggering receptor involved in tumor cell lysis by activated human natural killer cells, is a novel member of the immunoglobulin superfamily. *J Exp Med* **189**, 787-796 (1999).

25. Long, E.O. et al. Killer cell inhibitory receptors: diversity, specificity, and function. *Immunol Rev* **155**, 135-144 (1997).

26. Ruggeri, L. et al. Effectiveness of donor natural killer cell alloreactivity in mismatched hematopoietic transplants. *Science* **295**, 2097-2100 (2002).

27. Ruggeri, L. et al. Role of natural killer cell alloreactivity in HLA-mismatched hematopoietic stem cell transplantation. *Blood* **94**, 333-339 (1999).

28. Tam, Y.K., Miyagawa, B., Ho, V.C. & Klingemann, H.G. Immunotherapy of malignant melanoma in a SCID mouse model using the highly cytotoxic natural killer cell line NK-92. *J Hematother* **8**, 281-290 (1999).

29. Yan, Y. et al. Antileukemia activity of a natural killer cell line against human leukemias. *Clin Cancer Res* **4**, 2859-2868 (1998).

30. Tonn, T., Becker, S., Esser, R., Schwabe, D. & Seifried, E. Cellular immunotherapy of malignancies using the clonal natural killer cell line NK-92. *J Hematother Stem Cell Res* **10**, 535-544 (2001).

31. Berger, C. et al. Safety and immunological effects of IL-15 administration in nonhuman primates. *Blood* (2009).

32. Gong, J.H., Maki, G. & Klingemann, H.G. Characterization of a human cell line (NK-92) with phenotypical and functional characteristics of activated natural killer cells. *Leukemia* **8**, 652-658 (1994).

33. Sauce, D. et al. Influence of ex vivo expansion and retrovirus-mediated gene transfer on primary T lymphocyte phenotype and functions. *J Hematother Stem Cell Res* **11**, 929-940 (2002).

34. Grund, E.M. & Muise-Helmericks, R.C. Cost efficient and effective gene transfer into the human natural killer cell line, NK92. *J Immunol Methods* **296**, 31-36 (2005).

35. Hong, S. et al. Functional analysis of various promoters in lentiviral vectors at different stages of in vitro differentiation of mouse embryonic stem cells. *Mol Ther* **15**, 1630-1639 (2007).

36. Qin, J.Y. et al. Systematic comparison of constitutive promoters and the doxycycline-inducible promoter. *PLoS One* **5**, e10611 (2010).

37. Rosenberg, S.A., Restifo, N.P., Yang, J.C., Morgan, R.A. & Dudley, M.E. Adoptive cell transfer: a clinical path to effective cancer immunotherapy. *Nat Rev Cancer* **8**, 299-308 (2008).

38. Robbins, P.F. et al. Cutting edge: persistence of transferred lymphocyte clonotypes correlates with cancer regression in patients receiving cell transfer therapy. *J Immunol* **173**, 7125-7130 (2004).

39. Sambrook, J. & Russell, D.W. Molecular Cloning: A Laboratory Manual, Edn. 3. (Cold Spring Harbor Press, Cold Spring Harbor; 2001).

Supplementary Text 4.1

To decouple the relationship between transfection efficiency and the natural intensity of various fluorophores used in this study, transient transfections were performed in CTLL-2 cells—a cell line capable of relatively high transfection efficiencies by electroporation and is relatively insensitive to the specific expression vectors used compared to NK-92 cells—to compare the intensities of different GFP variants. Each fluorophore tested was expressed from a CMV promoter, and the following constructs were tested in parallel: a pcDNA3.1(+)-based plasmid encoding EGFP-T2A-IL2, a pcDNA3.1(+)-based plasmid encoding EGFP, and pmaxGFP encoding maxGFP. Transfection and flow cytometry analyses were performed as described in Chapter 3. Transfection results, in order of increasing fluorescence intensity, are as follows: EGFP-T2A-IL2, EGFP, and maxGFP (Supplementary Figure 4.1).

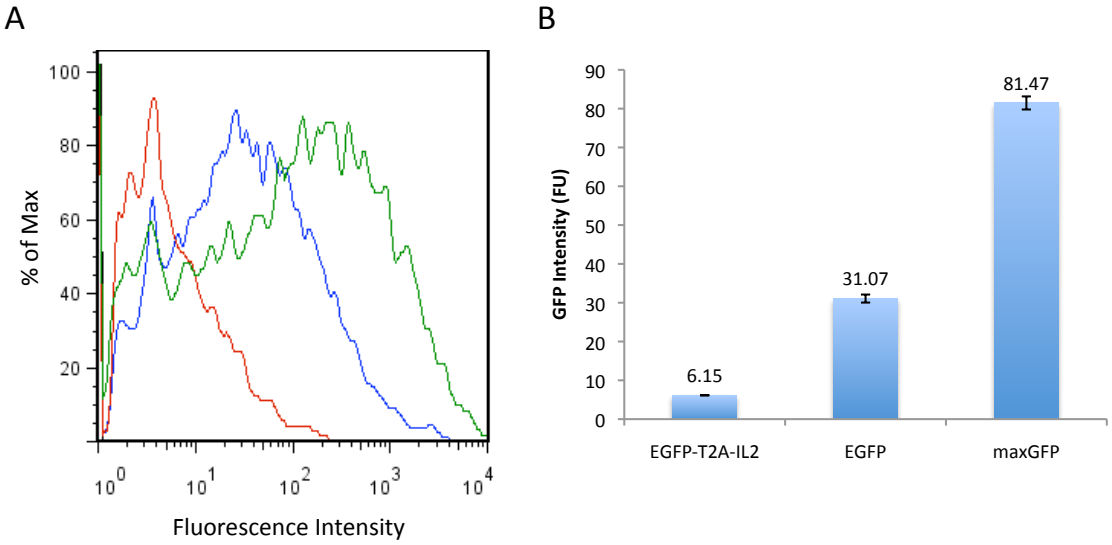

Supplementary Figure 4.1. Different GFP variants show different fluorescence intensities in transiently transfected CTLL-2 cells. (A) Fluorescence histogram of samples transiently transfected with various GFP reporters. Black, negative control (untransfected CTLL-2 cells); red, EGFP-T2A-IL2; blue, EGFP; green, maxGFP. (B) Geometric mean GFP intensity of viable, GFP^+ cells. Reported values are the mean of duplicate samples ± s.d.